TU Delft

Delft University of Technology

Analytical formulations and comparison of collapse models for risk analysis of axisymmetrically imperfect ring-stiffened cylinders under hydrostatic pressure

Reijmers, J. J.; Kaminski, M. L.; Stapersma, D.

DOI
10.1016/j.marstruc.2022.103161

Publication date
2022

Document Version
Final published version

Published in
Marine Structures

Citation (APA)
Reijmers, J. J., Kaminski, M. L., & Stapersma, D. (2022). Analytical formulations and comparison of collapse models for risk analysis of axisymmetrically imperfect ring-stiffened cylinders under hydrostatic pressure. *Marine Structures*, *83*, Article 103161. https://doi.org/10.1016/j.marstruc.2022.103161

Important note
To cite this publication, please use the final published version (if applicable).
Please check the document version above.

Copyright
Other than for strictly personal use, it is not permitted to download, forward or distribute the text or part of it, without the consent of the author(s) and/or copyright holder(s), unless the work is under an open content license such as Creative Commons.

Takedown policy
Please contact us and provide details if you believe this document breaches copyrights.
We will remove access to the work immediately and investigate your claim.

This work is downloaded from Delft University of Technology.
For technical reasons the number of authors shown on this cover page is limited to a maximum of 10.

Marine Structures 83 (2022) 103161

Contents lists available at ScienceDirect

Marine Structures

journal homepage: www.elsevier.com/locate/marstruc

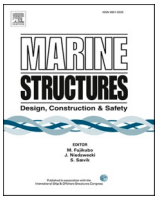

Analytical formulations and comparison of collapse models for risk analysis of axisymmetrically imperfect ring-stiffened cylinders under hydrostatic pressure

J.J. Reijmers *, M.L. Kaminski, D. Stapersma

Faculty of Mechanical, Maritime and Materials Engineering, Delft University of Technology, Mekelweg 2, 2628 CD, Delft, the Netherlands

ARTICLE INFO

Keywords:
Nonlinear finite element analysis
Submarine pressure hull
Ring-stiffened cylinder
Collapse

ABSTRACT

Risk-based design of marine pressure hulls require computationally efficient and precise models predicting collapse pressures of ring stiffened cylindrical shells as a function of realistic geometrical imperfections. However, the empirical interframe collapse models commonly implemented in design codes do not explicitly depend on imperfections, and the existing analytical models are only valid for axisymmetrically imperfect shells. The goal is to derive an analytical model that explicitly depends on axisymmetric and asymmetric imperfections. In order to derive such a model, first the stress development is investigated using the nonlinear Finite Element Analysis (FEA) of twelve marine pressure hulls having axisymmetric imperfections only. The knowledge gained from these investigations is used to qualify three collapse models. One of them, the integral model introduced by the authors, is accurate and sufficiently precise. It uses a new definition of interframe collapse, which also allows for asymmetric imperfections.

1. Introduction

Decision makers responsible for design, purchase, and operation of high-value assets, such as marine structures, need risk-based methods for comparing different alternatives and, subsequently, for making informed decisions. For ship and offshore structures such methods applied for structural systems have been discussed during the last ISSC congress [1]. These methods follow earlier developments for mechanical systems, e.g. Vucinic [2]. Recently Stambaugh [3] has presented and validated a new method that is based on a Risk and Total Ownership Cost (TOC) trade-space. The method can be used for making decisions on e.g.: carrying out a non-mandatory fatigue analysis, application of stricter or less stricter production tolerances, installing Hull Structural Monitoring (HSM), lifetime extension or selection of a new design from several alternatives. All these risk-based methods require, however, computationally efficient models capable of precisely predicting different structural failures.

This paper deals with submarine pressure hulls, consisting of a metallic cylindrical shell, stiffened by ring frames as shown schematically in Fig. 1. Its main structural failure is a collapse under external pressure which can be i) *interframe collapse*, i.e. collapse of shell between rings; ii) *global collapse*, i.e. bending collapse of ring stiffener including adjacent shell; iii) frame *tripping* and iv) failure of structural details (e.g. cone transitions, penetrations) (MacKay [4]). In general, the last two failure modes are avoided with a minor impact on pressure hull design by making their collapse pressures higher than the collapse pressures of the first two failure modes. The influence of frame tripping is in fact rather small [5] and the phenomenon can be avoided by imposing geometrical restrictions of ring

* Corresponding author.
E-mail address: j.j.reijmers-1@tudelft.nl (J.J. Reijmers).

https://doi.org/10.1016/j.marstruc.2022.103161
Received 20 August 2021; Received in revised form 26 November 2021; Accepted 11 January 2022
Available online 25 January 2022
0951-8339/© 2022 The Authors. Published by Elsevier Ltd. This is an open access article under the CC BY-NC-ND license (http://creativecommons.org/licenses/by-nc-nd/4.0/).

scantlings, which eliminate this failure mode. An example of such restrictions is given by Germanischer Lloyd [6]. This paper handles the interframe collapse.

Adequate models of the interframe collapse pressure for use in risk-based methods must be a function of scantlings, material data and fabrication factors such as geometrical imperfections, which can be axisymmetric or asymmetric.

The existing interframe collapse models are either empirical or analytical. Evidently empirical models based on statistical analysis of experimental data without explicit allowance for geometrical imperfections must be disqualified. As shown further on, and unfortunate for the purpose of present work, the main and widely used model of the *interframe* collapse pressure is an empirical model with scantlings and material data as input, leaving the imperfection unspecified. In contrast, the widely used model of the *global* collapse pressure explicitly allows for an asymmetric imperfection and, therefore, could be adequate for use in the risk-based methods.

There are analytical interframe collapse models, which are valid either for perfect or axisymmetric imperfect cylindrical shells supported by perfectly circular rings, Salerno and Pulos [7], Lunchick and Short [8] or for asymmetrically imperfect cylindrical shells supported by perfectly circular rings, Bodner and Berks [9], Kendrick [10], Galletly and Bart [11]. There are no analytical interframe collapse models known to the authors for axisymmetrically and asymmetrically imperfect cylindrical shells supported by imperfect (i.e. not perfectly circular) rings. The goal is to derive such a model and this paper describes first steps the authors have made towards this goal. These steps include i) collection of data on twelve sufficiently diverse marine pressure hulls; ii) interframe collapse analysis of these hulls with perfect and axisymmetrically imperfect cylindrical shells supported by perfectly circular rings using a nonlinear axisymmetric, i.e. 2D, Finite Element Analysis (FEA) which will be used as a reference for qualifying corresponding analytical interframe collapse models; iii) general discussion of existing interframe collapse models; iv) evaluation of existing analytical interframe collapse models for perfectly circular and axisymmetrically imperfect cylindrical shells supported by perfectly circular rings; and v) postulation of a new collapse model with a capability to allow for asymmetrically imperfect cylindrical shells and rings. The remaining steps will be reported in two follow-up papers and include vi) interframe collapse analysis of the hulls with asymmetrically imperfect cylindrical shells supported by perfectly circular and asymmetrically imperfect rings using a nonlinear 3D-FEA; and vii) qualification of the new model for such ring stiffened cylindrical shells.

The focus in qualifying different analytical collapse models is on their ability to allow for different imperfection forms. The FEA results are first used to determine the mean plastic reserve and the mean effect of imperfections. Subsequently the FEA calculations serve as a benchmark to qualify the analytical stress theories with respect to accuracy and precision in predicting first yield midbay. Finally, the FEA results are used to qualify the analytical collapse models regarding their accuracy and precision in predicting the interframe collapse pressures. The accuracy and precision both for first yield and interframe collapse were estimated by calculating a mean bias and its standard deviation for twelve hulls of sufficiently diverse geometries with either inner or outer rings. The best model for use in a risk analysis is a model having the highest precision, i.e. having the lowest standard deviation of its bias. The accuracy, i.e. the mean bias, is of less importance in a risk analysis because model predictions can be adjusted by using its value.

It is noted that the 2D-FEA results have been convincingly used as the reference because an additional investigation [12] has demonstrated that different FEA programs using different axisymmetric elements and meshes (Abaqus with elements CAX4R and CAX8R, NX NASTRAN with elements CQUADX4 and CQUADX8, and ANSYS with elements Plane182 and Plane183) give the same results when shear locking is prevented for linear elements. This means that the FEA predictions of the axisymmetric problem under consideration are deterministic, i.e. are free of uncertainty. An example of applied axisymmetric mesh with five quadratic higher order elements over the thickness is shown in Appendix A. For 3D-FEA it is different as shown by MacKay [13] and Reijmers and Stapersma [14].

2. Interframe collapse process

2.1. Perfect geometry

The process of interframe collapse of perfect ring stiffened cylindrical shells is discussed in this section. Submarine pressure hulls are stocky and their interframe collapse is dominated by plasticity before a significant geometrical nonlinearity is developed. This is hereafter illustrated using a non-linear FEA of twelve different pressure hulls described in Appendix A. These pressure hulls are characterised by three characteristic parameters (i.e. two parameters which are characteristic for the elastic buckling differential equation and one material parameter).

The first parameter is the shell flexibility parameter $\theta = \sqrt[4]{3\cdot(1-\nu^2)}\cdot L/\sqrt{R\cdot h}$ [7], also known in different forms as the Batdorf parameter $Z = \sqrt{1-\nu^2}\cdot L^2/(R\cdot h)$ [15] or the composite geometric parameter $S = \sqrt{6}/\pi\cdot\sqrt[4]{1-\nu^2}\cdot L/\sqrt{R\cdot h}$ [16]. Small (e.g. $Z < 10^2$)

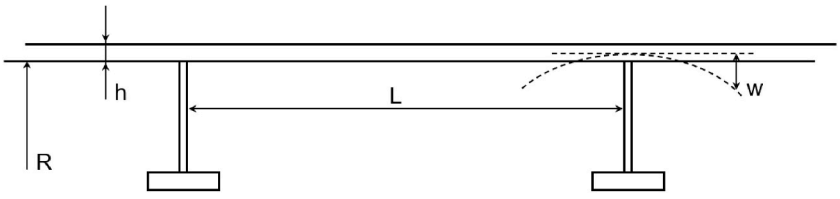

Fig. 1. A segment of a ring-stiffened cylindrical shell and its scantlings.

and high (e.g. $Z > 10^4$) values of these parameters indicate respectively a plate-like and a ring-like elastic buckling of cylindrical shells. As shown in the table in Appendix A all hulls under consideration have very small values of these parameters meaning that the cylindrical shells under consideration are short and would buckle like plates having the length (a) equal to shell's circumference ($a = 2\pi R$) and the width (b) equal to the cylindrical shell length ($b = L$).

The second parameter is the ratio of the shell area and the effective ring area A_s/A_f. This ratio controls the extent of buckling. The higher the ratio the smaller the rings and the more likely the global buckling and consequently the global collapse is. The table in Appendix A shows values of the ratio. The ratio is also plotted against the shell flexibility parameter in Fig. 2. The first seven hulls represent modern realistic submarine designs having relatively small values of the ratio indicating that they are designed to fail first by the interframe collapse. Remaining pressure hulls and especially both Kendrick hulls show higher values of the ratio indicating that they are designed to fail first by global collapse. Therefore, the paper presents two groups of statistical results: results calculated for all twelve hulls and the first seven.

The third parameter is a material parameter. It is the ratio between Young's modulus and the yield stress E/σ_y. This ratio controls the extent of yielding involved in a failure. The higher value of the ratio the more a structural failure is governed by yielding. All considered cylinders are made of materials having high values of the ratio. The table in Appendix A shows these values. Fig. 3 shows the ratio versus the shell flexibility parameter θ.

The pressures of first yield and the collapse pressures are given hereafter for all twelve hulls but the interframe collapse process is illustrated for the Starfish-aft hull only because the other hulls undergo a similar process. Fig. 4 shows how axial, hoop and von Mises stresses develop at the ring and midbay of the Starfish-aft hull. The blue and red lines indicate stress developments at outside and inside shell surfaces of the pressure hull, respectively. The relationship between stresses and external pressure is predominantly linear until the first yield occurs at the ring inside location at a pressure $p_{yy,ring} = 5.332$ MPa. This observation is important for analytical models discussed further on because it confirms that the nonlinear geometric effects are hardly developed when yielding starts for the hulls under consideration. The yielding zone at the ring extends slowly and yielding midbay at outside shell surface successively follows at a pressure $p_{yy,\ midbay} = 5.606$ MPa (The first yield pressure is calculated in pressure-von Mises space, as shown in Fig. 4e and f, by linear extrapolation of the last two solutions having von Mises stress lower than the yield stress.) The yielding zone midbay extends faster than the yielding zone at the ring and starts to dominate the interframe collapse process. At collapse pressure a large area midbay is yielding over the entire thickness, while at ring location the yield zone remains restricted to the inside of the shell. This justifies the assumption used in the analytical models as used by most Class Rules that interframe collapse is driven by yielding between the rings.

Further, all stresses at both locations begin as compressive stresses and remain compressive until yielding starts. During yielding some stress redistribution is taking place, which results in less compression midbay inside and a tension at ring outside location. This observation is also important for defining plastic hinges in analytical collapse models discussed further on. The collapse pressure of $p_c = 6.479$ MPa is defined as the last solution at which convergence criteria on displacements, forces and moments are met. The plastic reserve is defined as the ratio between the collapse pressure and the pressure at first yield at midbay and equals $p_c/p_{yy} = 1.16$. The results, including those for the other pressure hulls, are summarised in Table 1. The plastic reserve of all pressure hulls under consideration varies between 10% and 18%. The mean plastic reserve for all hulls and the first seven hulls do not differ much and equals 15% and 16%, respectively.

Next section presents the FEA results of the same pressure hulls but with an axisymmetrically imperfect cylindrical shells supported by perfectly circular rings.

2.2. Imperfect geometry

Submarine hulls show geometrical imperfections of their shells, caused by the fabrication process or operational incidents. The last ones (dents or locally reduced shell thickness caused by corrosion) result in an immediate repair or an operational restriction and are not considered in this paper. The fabrication induced shell imperfections are caused by welding of bended plates and ring stiffeners in

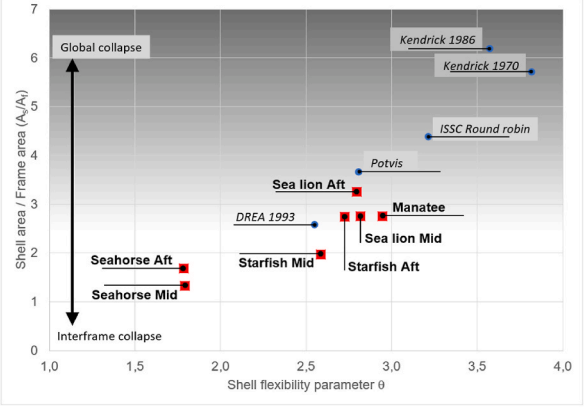

Fig. 2. Area ratio A_s/A_f versus shell flexibility parameter θ

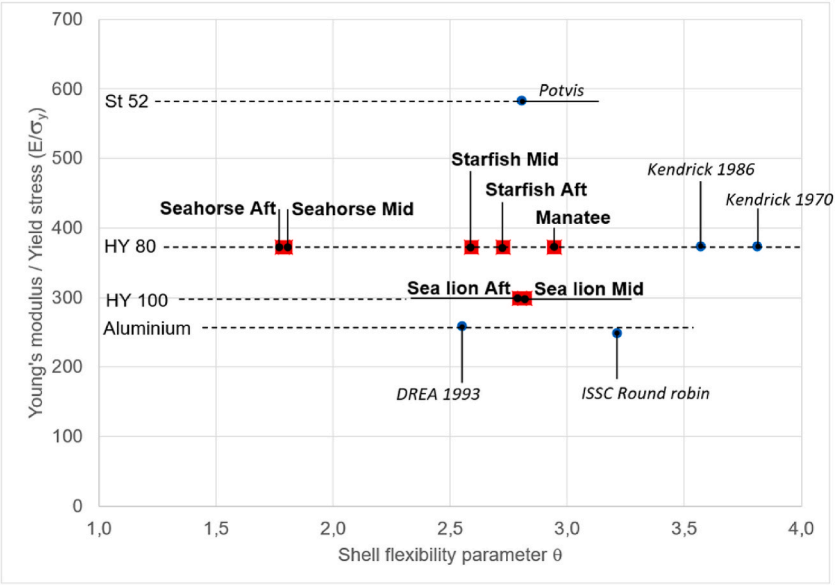

Fig. 3. Material parameter E/σ_y versus shell flexibility parameter θ

order to form a ring stiffened cylindrical shell.

Seams and welds of ring stiffeners induce predominantly axisymmetric imperfections which in the axial direction can be approximated by a half wave. This is in agreement with Ellinas and Croll [16] who predict such imperfections for ring stiffened cylindrical shells having composite geometric parameter $S < 2$, which is the case for the submarine pressure hulls under consideration (see the table in Appendix A) except the two Kendrick's hulls which have slightly higher values. It is important to note that with outer rings this axisymmetric imperfection will be directed outward, i.e. in the opposite direction to the deflection caused by the external pressure.

The butt welds between the bended plates of which the shell is fabricated induce an asymmetric imperfection showing N-waves in the circumferential direction, where N usually varies between 2 and 5. This imperfection spans over ring stiffeners and, therefore, also contributes to the global imperfection.

The classical elastic buckling theory states that only imperfections in the form of the lowest buckling mode reduce the elastic buckling pressure. For the pressure hulls under consideration the lowest interframe buckling pressure (listed in Appendix A) is much higher than the first yield pressure given in Table 1. The associated mode is asymmetric and shows n-waves around the circumference, where $n > N$ and ranges between 11 and 15 for the hulls under consideration as listed in Appendix A. An imperfection with such number of waves is in practice very small and is therefore disregarded. In this paper only axisymmetric shell imperfections are considered. However, the new interframe collapse model has a capability to account for asymmetric imperfections having N-waves.

The amplitude of the axisymmetric shell imperfection is chosen at L/250. This value is relatively high for submarine manufacturing but for the purpose of qualifying the model it approximately represents an average of maximum allowable amplitudes of axisymmetric shell imperfection (i.e. out-of-straightness) specified by the following codes:

- DNV-GL [17] and PD 5500 [18] specify maximum allowable amplitudes for long cylinders equal to L/500 and L/333, respectively.
- Offshore rules specify larger maximum allowable amplitudes, e.g. DNV–OS–C401 [19] specifies the amplitude equal to $\delta = 0.01$ g, where g is the rod length, which in the considered case equals the ring distance, giving the amplitude equal to L/100.
- Ellinas and Croll [16] base the amplitude on the composite geometry parameter S and this gives a varying percentage of the ring distance.

Table 2 summarises these amplitudes. Just for comparison, the last column of this table, gives the maximum allowable amplitude of asymmetric imperfection (i.e. out-of-circularity) specified in many codes.

Nevertheless, the goal is to show the interframe collapse process of axisymmetrically imperfect stocky shells and this should be qualitatively independent of imperfection amplitude in the range presented above. Following Lunchick and Short [8] the half wave shape of axisymmetric imperfection is modelled in a parabolic shape and, therefore, the initial imperfection has a discontinuity at ring location as shown for the *Starfish-aft* on Fig. 5a.

Fig. 5c and e shows how von Mises stresses develop midbay of the *Starfish-aft* and *Starfish-mid* having respectively outer and inner rings and having consequently opposite axisymmetric imperfections. Both developments are qualitatively the same and are also qualitatively the same to those developments shown in Fig. 4 for the perfect hull. Hence, all conclusions made for perfect hulls are also valid for imperfect hulls.

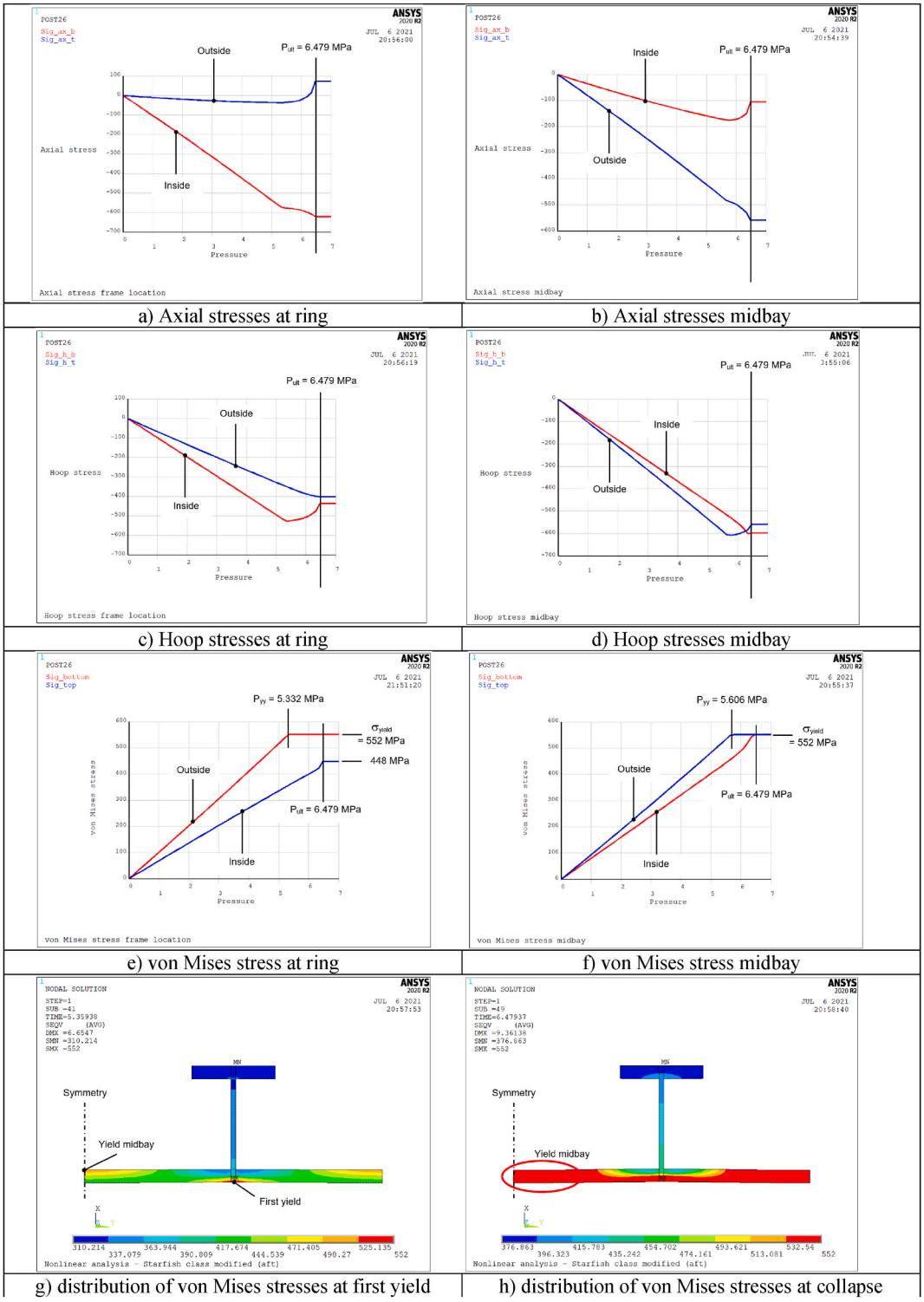

Fig. 4. FEA stress results for perfect Starfish-aft.

Table 3 shows the first yield and the collapse pressures for imperfect hulls. The mean plastic reserve of all pressure hulls under consideration (15%) and the first seven pressure hulls (16%) is the same as for perfect hulls. So, the selected amplitudes of axisymmetric imperfections do not affect plastic reserves.

Table 1
FEA pressure results for perfect hulls.

Perfect hull	First yield midbay pressure	Collapse pressure	Plastic reserve
	p_{yy}	p_c	p_c/p_{yy} - 1
	MPa	MPa	%
Manatee	5390	6290	17
Starfish - aft	5606	6479	16
Starfish - mid	5553	6570	18
Seahorse - aft	5956	6972	17
Seahorse - mid	5931	6759	14
Sea lion - aft	7371	8412	14
Sea lion - mid	7152	8313	16
Potvis	4896	5662	16
DREA experiment 1993	7825	9336	19
ISSC Round robin	7557	8637	14
Kendrick hull 1970	6064	6738	11
Kendrick hull 1986	5710	6290	10
	Mean plastic reserve	All geometries	15
		First seven	16

Table 2
Examples of maximum allowable axisymmetric and asymmetric imperfection amplitudes [mm].

Hull	Maximum allowable amplitude					
	Axisymmetric imperfection					Asymmetric imperfection
	DNV-GL L/500	PD 5500 L/333	DNV–OS–C401 L/100	Ellinas & Croll w_{max}	This paper L/250	PD 5500 DNV-GL 0.005*R_m
Manatee	1,30	1,95	6,50	7,40	2,60	15,1
Starfish - aft	1,25	1,88	6,25	6,97	2,50	15,6
Starfish - mid	1,60	2,40	8,00	8,67	3,20	21,1
Seahorse - aft	0,72	1,08	3,60	2,36	1,44	14,1
Seahorse - mid	0,90	1,35	4,50	2,97	1,80	17,6
Sea lion - aft	1,20	1,80	6,00	6,72	2,40	14,1
Sea lion - mid	1,50	2,25	7,50	8,43	3,00	17,6
Potvis	0,75	1,13	3,75	4,18	1,50	7,7
DREA experiment 1993	0,08	0,12	0,40	0,38	0,16	0,56
ISSC Round robin	0,10	0,15	0,50	0,55	0,20	0,61
Kendrick hull 1970	1,52	2,29	7,62	8,19	3,05	12,7
Kendrick hull 1986	1,46	2,19	7,30	8,09	2,92	13,5

2.3. Comparison between perfect and imperfect geometry

As expected, and as shown in Table 4, the first yield and the collapse pressures depend on the position of ring stiffeners. For hulls with inner and outer ring stiffeners the imperfections respectively decrease and increase both pressures. The change in the first yield pressure is −7.3 and 6.9% for inner and outer rings, respectively. The change in the collapse pressure −4.3 and 3.7% for inner and outer rings, respectively.

The qualitative and quantitative descriptions of the interframe collapse process of perfect and axisymmetrically imperfect hulls are hereafter used for qualifying corresponding analytical models. The 3D-FEA of interframe collapse of hulls having asymmetric shell imperfections with perfect and asymmetrically imperfect rings will be reported in two follow-up papers.

3. Pressure hull collapse models

Interframe buckling and collapse pressure models have a long history that dates to the beginning of the last century [20]. Over the 50's and 60's several models have been developed for estimating collapse pressures, and the achievements of the David Taylor Model Basin (USA) and the Naval Construction and Research Establishment (UK) contributed largely to present pressure hull design methods. Where the UK tradition for an important part makes directly use of experimental data through regression analysis, for instance Kendrick [21,22], Faulkner [23], Mackay [24], Cerik [25] and Cho [26], the US tradition relies mostly on analytical models presented by Salerno and Pulos [7], Galletly and Bart [11], Lunchick [27], Reynolds [28], Lunchick [29] and Pulos [30]. In 90's several researchers investigated probabilistic design of submarine pressure hulls among others Faulkner and Das [31], Faulkner [32], Chryssanthopoulos [33], Frieze [34], Morandi [35], Groen and Kaminski [36]. However, this research was focused on probabilistic design and was using existing analytical models. Therefore, this research is excluded from the discussion because it has not resulted in new

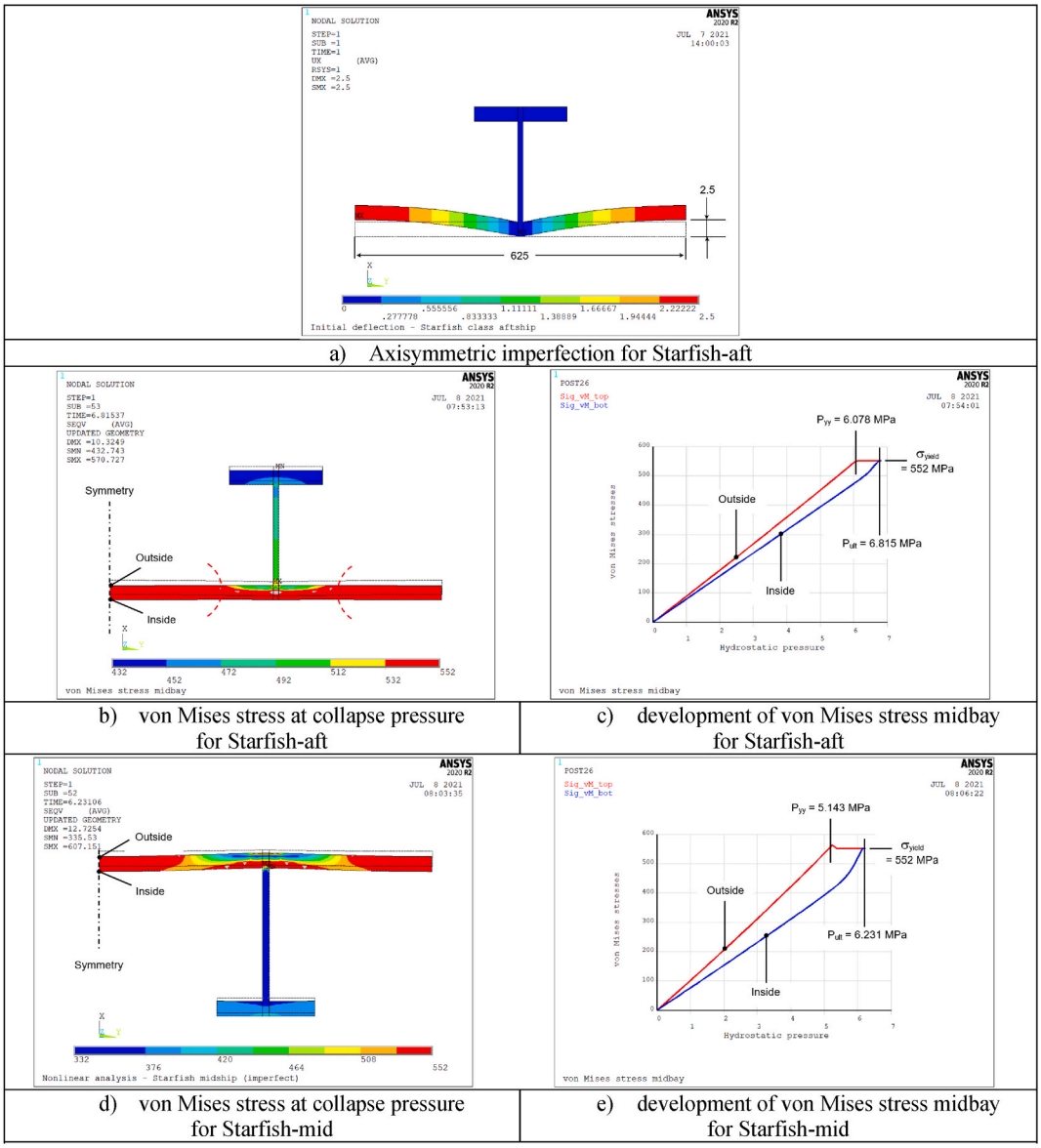

Fig. 5. FEA stress results for imperfect Starfish-aft and -mid.

interframe collapse models.

Until the last two decades interframe and global failure modes were assumed independent and assessed separately because the conventional design strategy was directed towards interframe collapse, i.e. a choice of the shell thickness, which predominantly defines the pressure hull mass, based on a safety factor on the axisymmetric stresses with respect to midbay yield, determined either in an empirical or analytical way. The global collapse pressure was kept away from the interframe collapse pressure by using a higher safety factor in order to account for a large uncertainty associated with interaction between both failure modes and large imperfection sensitivity of the global collapse pressure. A new design strategy, such as a Risk and TOC trade space, ultimately must account for possible interaction between both failure modes. However, first an interframe model, which explicitly accounts for both axisymmetric and asymmetric imperfections is needed.

4. Empirical interframe collapse models

An empirical interframe collapse pressure model is presented in the British Standard (BS) [18]. Its origin can be found in Ref. [21]. Kendrick presented his model to the British Standards institution in Ref. [22]. A thorough description is also given by Faulkner [23]. Fig. 6 shows a large collection of experimental data of interframe collapse pressures p_c which are normalized with the shell yield pressures p_y defined by Kendrick [22] (Section 8), i.e. a pressure at which the membrane hoop stress midbay reaches the minimum

Table 3
FEA pressure results for the imperfect hulls.

Hull with imperfection amplitude Lf/250	First yield midbay pressure p_{yy_i} MPa	Collapse pressure p_{c_i} MPa	Plastic reserve p_{c_1}/p_{yy_i} - 1 %
Manatee	4.994	5.947	19
Starfish - aft	6.078	6.815	12
Starfish - mid	5.143	6.231	21
Seahorse - aft	6.403	7.242	13
Seahorse - mid	5.497	6.647	21
Sea lion - aft	7.997	8.817	10
Sea lion - mid	6.626	7.863	19
Potvis	5.216	5.776	11
DREA experiment 1993	8.246	9.596	16
ISSC Round robin	7.218	8.412	17
Kendrick hull 1970	5.655	6.430	14
Kendrick hull 1986	6.199	6.570	6
	Mean plastic reserve	All geometries	15
		First seven	16

Table 4
FEA results – effect of imperfections on first yield and collapse pressures.

Hull	First yield pressure			Collapse pressure		
	Perfect	Imperfect	Difference	Perfect	Imperfect	Difference
(i) - inner ring	p_{yy}	p_{yy_i}	1 - p_{yy}/p_{yy_i}	p_c	p_{c_i}	1 - p_c/p_{c_i}
(o) - outer ring	MPa	MPa	%	MPa	MPa	%
Manatee (i)	5.390	4.994	−7,9	6.290	5.947	−5,8
Starfish - aft (o)	5.606	6.078	7,8	6.479	6.815	4,9
Starfish - mid (i)	5.553	5.143	−8,0	6.570	6.231	−5,4
Seahorse - aft (o)	5.956	6.403	7,0	6.972	7.242	3,7
Seahorse - mid (i)	5.931	5.497	−7,9	6.759	6.647	−1,7
Sea lion - aft (o)	7.371	7.997	7,8	8.412	8.817	4,6
Sea lion - mid (i)	7.152	6.626	−7,9	8.313	7.863	−5,7
Potvis (o)	4.896	5.216	6,1	5.662	5.776	2,0
DREA experiment 1993 (o)	7.825	8.246	5,1	9.336	9.596	2,7
ISSC Round robin (i)	7.557	7.218	−4,7	8.637	8.412	−2,7
Kendrick hull 1970 (i)	6.064	5.655	−7,2	6.738	6.430	−4,8
Kendrick hull 1986 (o)	5.710	6.199	7,9	6.290	6.570	4,3
		Mean difference (i)	−7,3			−4,3
		Mean difference (o)	6,9			3,7

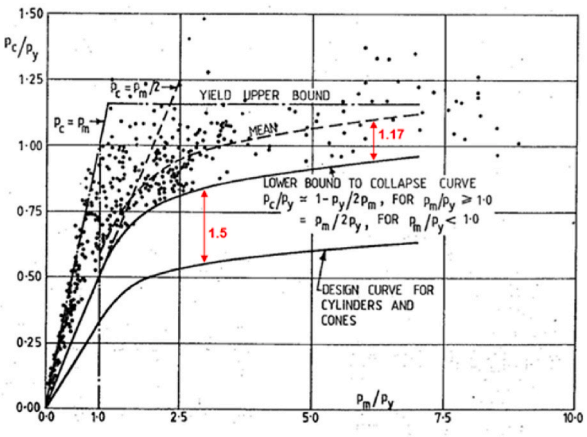

Fig. 6. Empirical basis of BS design curve for interframe collapse pressure (Faulkner, 1983, Image 4).

required yield stress. So, the contribution of the axial stress to the yielding is here disregarded. The ratio of p_c/p_y depends on the ratio p_m/p_y where p_m is the elastic interframe buckling pressure. This ratio presents a characteristic value of the pressure hull shell geometry. Hence, the empirical interframe model in PD 5500 depends solely on two variables p_m and p_y which do not depend on imperfections.

The effect of imperfections and other influencing parameters is considered by regression analysis of experimental results (as shown in Fig. 6) assuming that the experimental cylindrical shells had representative imperfections, i.e. out-of-circularity amplitude lower than R/200. PD 5500 uses a safety factor of 1.5 on the lower bound curve of empirical data of interframe collapse pressures whereas for global collapse pressures it uses a safety factor of 2.0. This difference in safety factors reflects Kendrick's intention of keeping global collapse pressures away from interframe collapse pressures.

Fig. 6 shows a significant scatter of the experimental data points. An analysis of graphically retrieved data gives the standard deviation of approximately 12%. Another estimate is published by Mackay [24] (his Table 2) who investigated the accuracy estimates for submarine design formulae. He estimated a coefficient of variation of 8.53% and a bias of 1.022 based on 50 experimental data points, resulting in a standard deviation of approximately 9%. Both standard deviations comprise measurement uncertainty, parameter uncertainty in scantlings, material properties and imperfections (i.e. deflections, misalignments, residual stresses) and model uncertainty caused by the assumed mean curve. The analytical models have no measurement uncertainty, use deterministic values of the parameters but have model uncertainty in the support by the ring stiffeners and in the collapse models. Therefore, the standard deviation in the comparison between analytical models and FEA results must be stricter than 9%–12%. In this paper the achievable standard deviation (precision) for three analytical collapse models will be assessed.

Besides the above empirical interframe collapse model, PD 5500 presents also an analytical interframe collapse model in Appendix M. This model will be discussed in a follow-up paper because this model is applicable for cylindrical shells with asymmetrically imperfect shells with imperfection amplitudes higher than R/200 and perfectly circular rings.

PD 5500 [18] without its Appendix M is an example of a conventional design methodology with an empirical model for the interframe collapse pressure. This disqualifies PD 5500 design methodology for an adequate use in risk-based methods.

Cerik [25] eliminates the separate treatment of interframe and global failure modes by proposing the following interaction formula:

$$\left(\frac{p_c}{\rho_1 \cdot p_m} + \frac{p_c}{\rho_{oa} \cdot p_n}\right)^2 + \left(\frac{p_c}{p_{yy}}\right)^2 = 1 \tag{1}$$

where p_c is a collapse pressure in an undefined mode, p_m is the linear elastic interframe buckling pressure defined by von Mises [37], p_n is the linear elastic global buckling pressure presented by Bryant [38], and ρ_1 and ρ_{oa} are knockdown factors which are determined in a regression analysis of experimental data and implicitly account for effects of interframe and global imperfections, respectively. Cerik defines the yield pressure p_{yy} as the pressure causing yield midbay at the shell centre. He uses therefore the equivalent stress calculated from the hoop membrane stress and the axial membrane stress (Equation (5)).

It is observed that Cerik's formula (1) does not reduce to the formulation of PD 5500 for the interframe collapse pressure shown in Fig. 6, when p_n is disregarded, $p_m/p_y \gg 1$ and when p_y is used instead of p_{yy}.

The Cerik's model is an empirical combination model of both collapse modes that not really explains the interaction and does not explicitly depend on interframe imperfections. This disqualifies the model for use in risk-based methods. The same conclusion applies for the model presented by Cho [26] who extended Cerik's model by accounting for the ring tripping failure mode. Hence there will be a need of proposing a new combined model which will be a function of the global collapse pressure and a new interframe collapse pressure model presented in this and follow-up papers.

5. Analytical interframe collapse models

5.1. Axisymmetric stress theory

Stress levels in perfectly circular, ring-stiffened cylindrical shells were given by von Sanden and Günther [39] and improved by Salerno and Pulos [7]. They derived the solution for a fourth order differential equation in radial deflection of a thin-walled cylindrical shell including geometrically nonlinear terms coupling radial deflection with axial compression, i.e. the beam-column effect. The ring-frame was considered as a boundary condition with constrained rotation and finite radial stiffness determined by the area of the ring. The ring area is translated into an effective area depending on the location of the ring (inside or outside) where the dependency on the ratio of the radii of the shell and the centre of gravity (C.o.G.) of the ring can be either linear or quadratic. Where Salerno and Pulos [7] leave the choice between linear or quadratic dependency open (see their equation 24), Pulos [30] states that linear dependency is applicable to internal rings and quadratic dependency to external rings (see his equation 9). Kendrick [21] following Wilson [40] (1966) has the quadratic relation. In this paper a linear dependency is used. The solution basically gives the radial deflection, and this means that the decrease in radius gives not only the stresses in the shell (both midbay and at ring location) but also the stresses in the rings. Different codes are based on their solution. While DNV-GL follows the same solutions as the authors, PD 5500 (in 3.6.2.1) uses the solution without the beam-column effect and with the quadratic dependency. The solution shows that normally first yield in the shell occurs at ring location at the inner side of the shell, followed by yielding midbay at the outer side. This matches very well FEA results presented earlier.

Following the solution of Salerno and Pulos [7] for a perfect cylindrical shell Lunchick & Short [8] presented an analytical solution

for cylindrical shells having axisymmetric imperfections described by a parabolic shape between the rings.

Table 5 shows the pressures giving first yield for the perfect (S&P) and the imperfect (L&S) hulls. These pressures are compared with the FEA result presented in Table 4. The first seven geometries are considered to be realistic modern pressure hull designs and show a small bias (−0.16% for the perfect hull and −0.22% for the imperfect hull). Both stress theories are precise because the standard deviations (0.6% and 0.7%) are very low.

5.2. Mid-fibre yield pressure collapse model (MYP)

Salerno and Pulos [7] proceed further and present a simple approach to collapse of a perfect cylindrical shell (see their equation 98) considering only the mid-fibre (membrane) stress of the solution described above. Collapse is assumed when the von Mises stress at mid-fibre between the rings reaches the yield stress indicating that half of the shell thickness must be yielding as indicated by the red zone in Fig. 7, although the exact behaviour in the plastic zone is not considered. The interframe collapse pressure model of Salerno and Pulos (the MYP model) does not allow for imperfections but in case of axisymmetric imperfections the stress state at first yield according to Lunchick and Short (L&S) can be applied.

For comparison with other models the mid-plane yield predictions are compared separately for all geometries, the first seven (being realistic pressure hull designs) in Table 6. The model gives good predictions of the collapse pressures. The mean bias calculated for all hulls under consideration is 1.7% for the perfect hull and 1.6% for the imperfect hull. For the first seven hulls the mean bias is even lower and equals −0.2% and −0.4%, respectively. The difference in collapse pressures is caused by their different definitions. For the S&P-model the yielding of half of the thickness is sufficient whereas in FEA the yielding develops further until lack of convergence.

Table 6 also gives the standard deviation of the biases. This because, in addition to allowance for imperfections, the standard deviations of the biases are used for qualifying different analytical models. The realistic geometries, presented by the first seven, show a standard deviation of 2.2% for the perfect hull and 3.4% for the hull with initial imperfection. This means that the precision is better than the 5% following from the experimental results (see Fig. 6).

5.3. Plastic hinge collapse model (HIN)

Lunchick [27] used stress formulas derived by Salerno and Pulos [7] and defined the interframe collapse mechanism as beginning of a plastic hinge at midbay. He assumed the stress state in a plastic hinge at midbay, as shown in Fig. 8, in which the outer side of the shell is in axial and circumferential directions in compression, and the inner side of the shell is in both directions in tension. This assumption is not valid for hulls under consideration because hoop stresses are always in compression at both sides of the shell as shown in Fig. 4.

Nevertheless his analytical derivations are correct. His formulation assumes a linear relation between hydrostatic pressure and resulting sectional forces and moments and thus stress, midbay in axial and circumferential direction. This means that linearity is assumed not only in the elastic range, but also in the plastic range as Lunchick clearly states. Fig. 9 shows the stress distribution over the thickness at first yield and collapse. Both distributions are proportional to the hydrostatic pressure. Although at some locations the yield stress is exceeded it is assumed that the distribution of stress is not affected and increases linearly with the pressure. This linearity also neglects the beam-column effect, which introduces a nonlinear relation between pressure and stress. Since the beam-column effect already occurs in the elastic regime, it is best to determine the linear relations at the pressure inducing first yield midbay at the outside

Table 5
First yield pressure for the perfect hull and the hull with imperfection.

First yield midbay	Perfect hull			Imperfection amplitude		$L_f/250$
	S&P	FEA	(FEA-S&P)/FEA	L&S	FEA	(FEA-L&S)/FEA
	p_y	p_y		p_y	p_y	
Geometry	MPa	MPa	%	MPa	MPa	%
Manatee	5.380	5.390	0,2	4.995	4.994	0,0
Starfish - aft	5.586	5.606	0,4	6.043	6.078	0,6
Starfish - mid	5.569	5.553	−0,3	5.174	5.143	−0,6
Seahorse - aft	6.025	5.956	−1,1	6.440	6.403	−0,6
Seahorse - mid	5.969	5.931	−0,6	5.569	5.497	−1,3
Sea lion - aft	7.345	7.371	0,4	7.946	7.997	0,6
Sea lion - mid	7.147	7.152	0,1	6.640	6.626	−0,2
Potvis	4.876	4.896	0,4	5.183	5.216	0,6
DREA experiment 1993	7.981	7.825	−2,0	8.375	8.246	−1,6
ISSC Round robin	7.418	7.557	1,8	7.099	7.218	1,6
Kendrick hull 1970	6.015	6.064	0,8	5.611	5.655	0,8
Kendrick hull 1986	5.650	5.710	1,0	6.127	6.199	1,2
Mean bias		All	0,1		All	0,1
		First seven	−0,2		First seven	−0,2
Standard deviation		All	1,0		All	1,0
		First seven	0,6		First seven	0,7

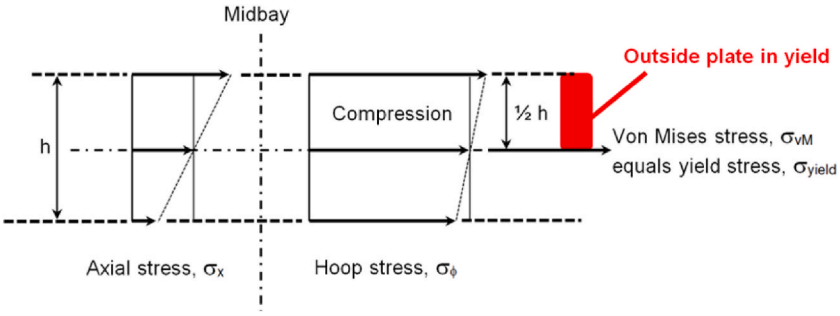

Fig. 7. MYP model – assumed stress distribution midbay at collapse pressure.

Table 6
Comparison Mid-fibre Yield Pressure collapse (MYP) with FEA result.

Collapse model	Perfect hull			Imperfection amplitude		$L_f/250$
(MYP)	MYP	FEA	(FEA-MYP)/FEA	MYP	FEA	(FEA-MYP)/FEA
	p_c	p_c		p_c	p_c	
Geometry	MPa	MPa	%	MPa	MPa	%
Manatee	6.224	6.290	1,1	5.998	5.947	−0,9
Starfish - aft	6.437	6.479	0,7	6.652	6.815	2,4
Starfish - mid	6.687	6.570	−1,8	6.488	6.231	−4,1
Seahorse - aft	6.859	6.972	1,6	6.945	7.242	4,1
Seahorse - mid	7.062	6.759	−4,5	6.968	6.647	−4,8
Sea lion - aft	8.322	8.412	1,1	8.611	8.817	2,3
Sea lion - mid	8.287	8.313	0,3	8.005	7.863	−1,8
Potvis	5.363	5.662	5,3	5.504	5.776	4,7
DREA experiment 1993	9.056	9.336	3,0	9.220	9.596	3,9
ISSC Round robin	8.121	8.637	6,0	7.938	8.412	5,6
Kendrick hull 1970	6.462	6.738	4,1	6.170	6.430	4,0
Kendrick hull 1986	6.061	6.290	3,6	6.358	6.570	3,2
Mean bias		All	1,7		All	1,6
		First seven	−0,2		First seven	−0,4
Standard deviation		All	3,0		All	3,6
		First seven	2,2		First seven	3,4

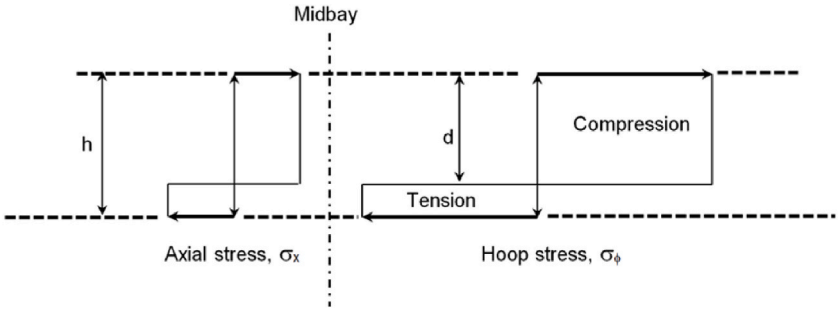

Fig. 8. Lunchick's assumed stress distribution in a plastic hinge a midbay.

side of the shell. Fig. 9 show stress levels for the Starfish-aft over the shell thickness at first yield pressure of $p_{yyS\&P} = 5.586$ MPa. Based on these stress levels the Lunchick's model gives the collapse pressure of $p_{cHIN} = 6.145$ MPa. Fig. 9 further illustrates how von Mises stress is distributed over the shell thickness at first yield midbay and at the collapse pressure as defined by Lunchick. From the definition of von Mises stress $\sigma_{vM} = \sqrt{\sigma_{ax}^2 + \sigma_{\varphi}^2 - \sigma_{ax} \cdot \sigma_{\varphi}}$ follows that von Mises stress is also linear with the hydrostatic pressure, p, however, it is nonlinearly distributed over the shell thickness coordinate z. The property that von Mises stress is proportional with the external pressure is further on used for derivation of a new model for the interframe collapse model.

The Lunchick's interframe collapse model is denoted by HIN and predictions are compared with FEA results in Table 7. The mean bias of the collapse pressure predicted by the HIN model is much higher than found by the MYP model. Considering all the twelve

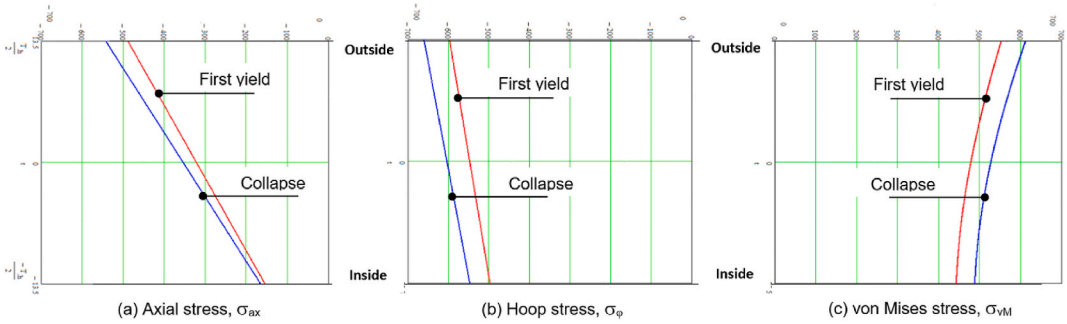

Fig. 9. Stresses over the thickness midbay – Starfish aft hull.

Table 7
Comparison Plastic Hinge (HIN) with FEA result.

Collapse model	Perfect hull			Imperfection amplitude		$L_f/250$
(HIN)	HIN	FEA	(FEA-HIN)/FEA	HIN	FEA	(FEA-HIN)/FEA
	p_c	p_c		p_c	p_c	
Geometry	MPa	MPa	%	MPa	MPa	%
Manatee	5.939	6.290	5,6	5.651	5.947	5,0
Starfish - aft	6.145	6.479	5,2	6.447	6.815	5,4
Starfish - mid	6.289	6.570	4,3	6.005	6.231	3,6
Seahorse - aft	6.562	6.972	5,9	6.771	7.242	6,5
Seahorse - mid	6.660	6.759	1,5	6.433	6.647	3,2
Sea lion - aft	7.995	8.412	5,0	8.391	8.817	4,8
Sea lion - mid	7.902	8.313	4,9	7.533	7.863	4,2
Potvis	5.198	5.662	8,2	5.396	5.776	6,6
DREA experiment 1993	8.680	9.336	7,0	8.929	9.596	7,0
ISSC Round robin	7.885	8.637	8,7	7.654	8.412	9,0
Kendrick hull 1970	6.322	6.738	6,2	5.995	6.430	6,8
Kendrick hull 1986	5.931	6.290	5,7	6.284	6.570	4,4
Mean bias		All	5,7		All	5,5
		First seven	4,6		First seven	4,7
Standard deviation		All	1,9		All	1,7
		First seven	1,5		First seven	1,1

geometries the mean bias is more than 3 times higher for the perfect hulls (5.7/1.7) and also for the imperfect hulls (5.5/1.6). This inaccuracy can be eliminated in a risk analysis by correcting the HIN model predictions with the mean bias. The standard deviation of the collapse pressure bias is for the HIN model lower than for the MYP model. For all twelve geometries the standard deviation for the perfect hull is 1.9% versus 3.0% and for the imperfect hull 1.7% versus 3.6%. Therefore, for the risk-based methods the HIN model formally is more attractive than the MYP model, in spite of its doubtful mechanism and large bias.

5.4. Integral collapse model (INT)

From Table 5 follows that elastic stress solutions of Salerno and Pulos [7] and Lunchick and Short [8] for respectively perfect and axisymmetrically imperfect ring stiffened cylindrical shells are accurate and precise. This supports the choice of both stress solutions as a basis for the new model. What remains is to define the collapse pressure in such a way that it depends on additional stresses caused by asymmetric imperfections of shell and rings. These additional stresses will be investigated in follow-up papers. The present paper develops a new method to define the collapse pressure and validates the new model for perfect and axisymmetrically imperfect ring stiffened cylindrical shells.

Considering the membrane stresses only when defining the collapse pressure would probably not work because the additional bending hoop stress due to asymmetric imperfection influences the membrane stresses throughout the geometric nonlinearity which is not significant for the pressure hulls under consideration. As it will be demonstrated, a better choice is connecting the collapse pressure with yielding of the whole shell thickness midbay, i.e. $\sigma_{vM} = \sigma_y$ at each z position. As there is no elastic-plastic stress solution available for pressures higher than the first yield pressure an engineering approach is followed.

First the elastic Salerno and Pulos [7] solution for perfect hulls is used in order to calculate the hoop and axial stresses midbay. Second, the first yield pressure midbay is determined $p_{yyS\&P}$. Then, von Mises stresses over the shell thickness midbay at onset of yielding $\sigma_{vM}(z, p = p_{yyS\&P})$ are calculated. After that, the earlier discussed property that von Mises stress is proportional to the pressure is used. So, it is assumed that at the onset of yielding the ratio of the first yield pressure and an integral of von Mises elastic stresses over

the shell thickness equals the ratio of collapse pressure and an integral of yield stress over the shell thickness (indicating yielding over whole shell thickness):

$$\frac{p_{yyS\&P}}{\int_{-h/2}^{h/2}\sigma_{vM}\left(z,p=p_{yyS\&P}\right)dz}=\frac{p_{cI}}{\int_{-h/2}^{h/2}\sigma_y dz} \tag{2}$$

The above equation gives the interframe collapse pressure for perfect ring stiffened cylindrical shells as:

$$p_{cI}=\frac{h\cdot\sigma_y}{\int_{-h/2}^{h/2}\sigma_{vM}\left(z,p=p_{yyS\&P}\right)dz}p_{yyS\&P} \tag{3}$$

The above new model is called the *Integral* model, i.e. the INT model, because the collapse pressure is predicted using two stress integrals. For axisymmetrically imperfect hulls the *Lunchick and Short* stress solution is used and then the interframe collapse pressure for axisymmetrically imperfect hulls equals:

$$p_{cIl}=\frac{h\cdot\sigma_y}{\int_{-h/2}^{h/2}\sigma_{vM}\left(z,p=p_{yyL\&S}\right)dz}p_{yyP} \tag{4}$$

Both equations (3) and (4) use elastic stress solutions and do not require elastic-plastic calculations. Before qualifying the INT model, first an example is given in order to quantitatively illustrate the new definition. The example concerns application of Equation (3) for the perfect Starfish-aft. Fig. 10 shows the distribution of von Mises stresses over the thickness midbay when the first yield takes place at outside shell midbay at pressure $p_{yyS\&P}=5.586$ MPa. This distribution is obtained using the Salerno and Pulos stress solution. The integral of these stresses equals:

$$\int_{-h/2}^{h/2}\sigma_{vM}\left(z,p=p_{yyS\&P}\right)dz=13,066\ MPa\cdot mm \tag{5}$$

The integral of the yield stress over the thickness equals:

$$h\cdot\sigma_y=27\ mm\cdot 552\ MPa=14,904\ MPa\cdot mm \tag{6}$$

Hence, the collapse pressure for the perfect Starfish-aft equals:

$$p_{cI}=\frac{14,904\ MPa\cdot mm}{13,066\ MPa\cdot mm}5.586\ MPa=6.371\ MPa \tag{7}$$

Fig. 10 also demonstrates the difference between the MYP model and the INT model. The dashed red line shows von Mises stresses equal to the yield stress at each z what corresponds to a fully plastic shell thickness. The continuous red line shows hypothetical von Mises stresses calculated using elastic Salerno and Pulos solution if no plasticity would occur and the area under both red lines is equal. Because of the concave distribution of the von Mises stress over the thickness its value at the shell centre is just below yield. This is

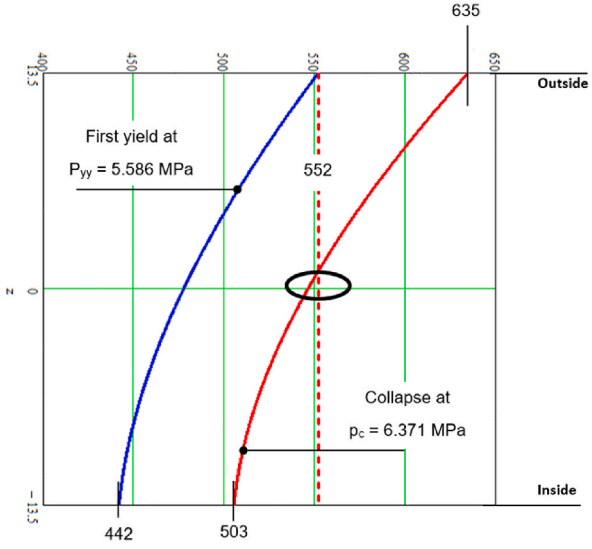

Fig. 10. Von Mises stress distribution over the thickness midbay at first yield pressure (blue) and at collapse pressure (red) for Starfish-aft.

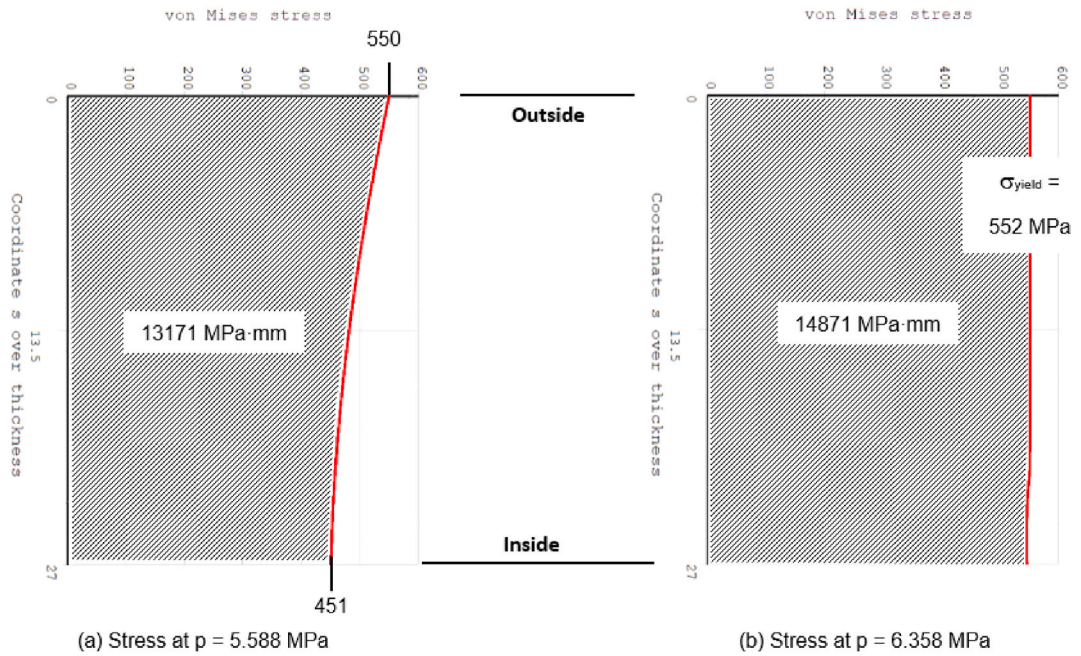

Fig. 11. FEA results for Starfish-aft, von Mises stress distribution over the thickness midbay at a) first yield pressure, and b) at collapse pressure.

encircled by a black ellipse on Fig. 10. This means that the INT model gives lower collapse pressures than the MYP model, which requires the yield pressure at the shell centre. This difference is desired because MYP model gives not conservative results for Starfish-mid and Seahorse-mid.

Now the new definition of the interframe collapse pressure is compared with the FEA results. Fig. 11 shows two von Mises stress distributions over the thickness obtained from FEA of Starfish-aft. The left one is at the load step near the first yield pressure midbay (i.e. $p_{yy} = 5.586$ MPa, see Table 5). The right one is at the load step near the collapse pressure (i.e. $p_c = 6.371$ MPa, see equation (7)). The integrals of both distributions equal 13,171 MPa mm and 14,871 MPa mm, respectively. Their ratio equals 1.1291. The analytical integrals are given in Equations (5) and (6), and their ratio equals 1.1407. The difference between both ratios equals 1.0% in this case and underpins the new analytical definition of the collapse pressure. A next support of the definition is given in Fig. 12 which compares the variation of the von Mises stress integral with the external pressure obtained from the FEA with the linear variation assumed in the definition.

Fig. 12 confirms that the FEA results vary almost linearly up to the analytical collapse pressure. This justifies the assumption made in the new definition that in excess of the first yield pressure the integral of the von Mises stress over the thickness varies linearly with the pressure.

Having examined the new collapse definition, the remaining part of this section qualifies the new integral model based on its predictions for the twelve pressure hulls under consideration.

The INT model predictions for perfect hulls and hulls with imperfection are compared with FEA results in Table 8. The accuracy of the INT model, represented by the mean bias, regarding the collapse pressure is 2.5% for all perfect hulls and hulls with imperfection. This is better than mean biases of the HIN model (5.7% and 5.5%) and somewhat worse than mean biases of the MYP model (1.7% and 1.6%). These differences are less relevant in the risk analysis because model predictions can be corrected by using its mean bias. More relevant is the model precision represented by the standard deviation of the bias. The precision of the INT model regarding the collapse pressure equals 2.7% and 2.9% for all perfect hulls and the imperfect hulls, respectively.

Considering the first seven geometries, which can be addressed as realistic designs, the standard deviation is even lower. These geometries show 2.1% and 2.7% for respectively the perfect and imperfect hulls. This is better than the MYP model (2.2% and 3.4%) but worse than the HIN model (1.5% and 1.1%). Nevertheless, the INT model meets the requirement that its precision must be stricter than the 5% following from the experiments.

The next section summarises all findings in successive evaluations of the three collapse models.

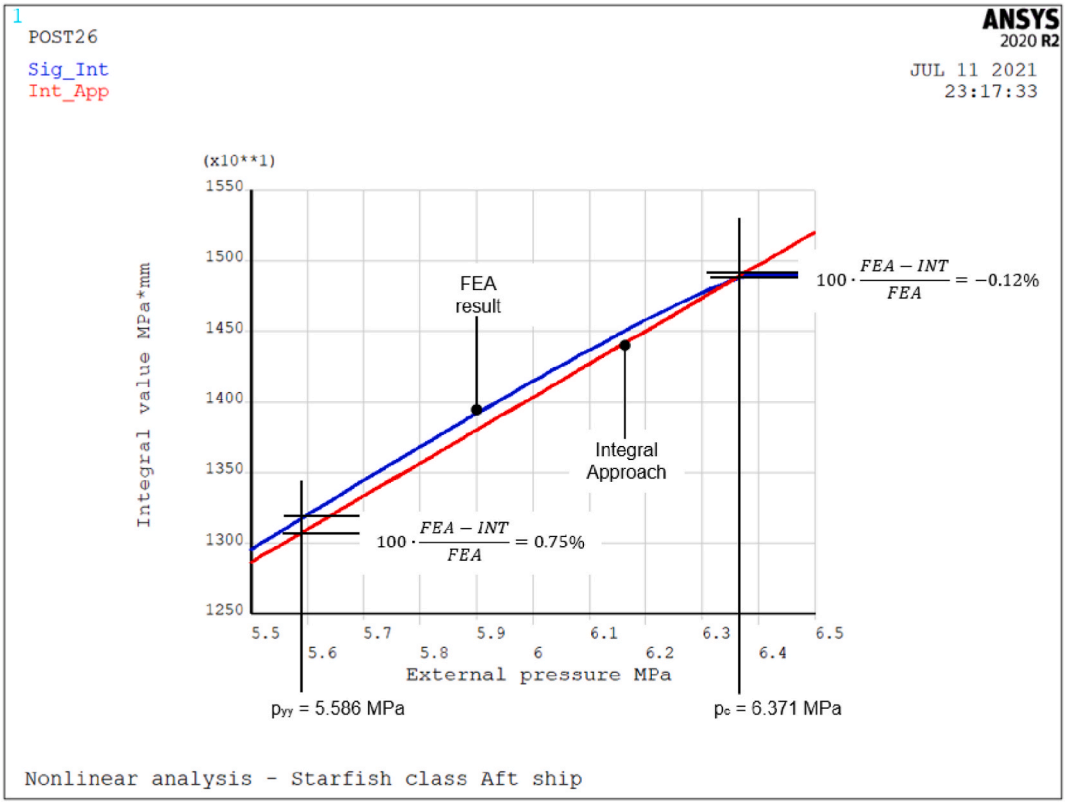

Fig. 12. Comparison of INT model and FEA – for perfect Starfish-aft.

Table 8
Comparison Integral model (INT) with FEA result.

Collapse model	perfect hull			Imperfection amplitude		$L_f/250$
(INT)	INT	FEA	(FEA-INT)/FEA	INT	FEA	(FEA-INT)/FEA
	p_c	p_c		p_c	p_c	
Geometry	MPa	MPa	%	MPa	MPa	%
Manatee	6.157	6.290	2,1	5.891	5.947	0,9
Starfish - aft	6.371	6.479	1,7	6.621	6.815	2,8
Starfish - mid	6.592	6.570	−0,3	6.340	6.231	−1,8
Seahorse - aft	6.815	6.972	2,3	6.930	7.242	4,3
Seahorse - mid	6.999	6.759	−3,5	6.855	6.647	−3,1
Sea lion - aft	8.252	8.412	1,9	8.582	8.817	2,7
Sea lion - mid	8.200	8.313	1,4	7.865	7.863	0,0
Potvis	5.329	5.662	5,9	5.490	5.776	4,9
DREA experiment 1993	8.980	9.336	3,8	9.176	9.596	4,4
ISSC Round robin	8.077	8.637	6,5	7.872	8.412	6,4
Kendrick hull 1970	6.438	6.738	4,5	6.128	6.430	4,7
Kendrick hull 1986	6.040	6.290	4,0	6.352	6.570	3,3
Mean bias		All	2,5		All	2,5
		First seven	0,8		First seven	0,8
Standard deviation		All	2,7		All	2,9
		First seven	2,1		First seven	2,7

Table 9
Overview of analytical interframe collapse models – bias with respect to FEA.

Model		All twelve hulls		First seven hulls		Allowance for asymmetric imperfection
		Mean bias	SD	Mean bias	SD	
		%	%	%	%	
Perfect hulls	MYP	1,7	3,0	−0,2	2,2	No
	HIN	5,7	1,9	4,6	1,5	No
	INT	2,5	2,7	0,8	2,1	Yes
Hulls with imperfection	MYP	1,6	3,6	−0,4	3,4	No
	HIN	5,5	1,7	4,7	1,1	No
	INT	2,5	2,9	0,8	2,7	Yes

6. Discussion and conclusions

This paper qualifies two existing and one new analytical interframe collapse models of ring stiffened cylindrical shells for use in the risk-based analyses. The collapse models are based on stress levels following from axisymmetric stress theory. Table 5 presents a comparison between the results from this theory and FEA results and for the realistic pressure hull designs the precision is lower than 1%.

Table 9 gives an overview of the three collapse models where the last collapse model (INT) is introduced in this paper. Since this model considers the stress distribution over the complete thickness of the hull it allows not only for axisymmetric imperfection but also for asymmetric imperfection (Out-of-Circularity). The application and qualification of the INT model for asymmetric imperfection will be reported in follow-up papers.

The overview in Table 9 presents the mean value of the biases and the standard deviations. Especially the standard deviations are of interest since they show the precision of the models. The mean of the bias can be corrected by a factor in risk-based design. This suggests that the HIN model performs better since the standard deviation (precision) has the lowest values. However the HIN model has a doubtful basis since a plastic hinge is not developed. The outside of the hull midbay starts to yield and plasticity develops over the thickness and then from midbay towards the rings. The assumed tension at the inside of the shell is not found. Considering the additional bending stress in case of asymmetric imperfection (out-of-circularity) the HIN model will not be able to cope with the stress distribution over the thickness. The same applies to the MYP model. Since only mid-fibre stresses at the plate centre are considered the additional bending is not covered.

The integral model (INT) shows a better precision than the MYP model but worse than the HIN model. The objective was a better precision than the 9%–12% found for the empirical method presented in section 4. This is achieved by the analytical INT model with a maximum value of 2.7% for the imperfect hull and considering only the realistic designs. But most importantly the INT model, making use of the full stress distribution, can allow for asymmetric imperfections.

Declaration of competing interest

The authors declare that they have no known competing financial interests or personal relationships that could have appeared to influence the work reported in this paper.

Appendix A

Table A-1 shows the data for the twelve geometries presented in this paper. These geometries are divided in seven representative designs (shown in Figure A.1) and five additional ones in Figure A.2.

Table A-1 is split in four parts and the first part shows the dimensions of the pressure hull and the material properties. Some derived dimensions which are entered in the analytical formulations can be found in the second part. The third part contains the non-dimensional parameters that characterize the different geometries. The last row presents the linear elastic buckling pressure according to von Mises as a reference.

Table A-1
Overview of the geometries under consideration

		Manatee	Starfish Aft	Starfish Mid	Seahorse Aft	Seahorse Mid	Sea lion Aft	Sea lion Mid	Potvis	DREA experiment 1993	ISSC Round robin	Kendrick 1970	Kendrick 1986
Frame position	–	Inner	Outer	Inner	Outer	Inner	Outer	Inner	Outer	Outer	Inner	Inner	Outer
Inner radius	mm	3000	3100	4200	2800	3500	2800	3500	1540	110	120	2527	2688
Hull thickness - h	mm	26	27	36	22	27	26	32	18	2,7	3	25,4	25
Frame distance	mm	650	625	800	360	450	600	750	375	40	50	762	730
Frame web height	mm	175	190	320	170	230	160	200	124.5	8	8	187	190
Frame web thickness	mm	9	10	16	15	20	12	14	10	5,5	2	8128	8
Frame flange width	mm	120	175	235	110	150	120	170	46	–	8	101,6	100
Frame flange thickness	mm	35	27	36	22	27	26	32	15.5	–	2	16,26	16
Material	–	HY80	HY80	HY80	HY80	HY80	HY100	HY100	St52	Al	Al	HY80	HY80
Yield stress	MPa	552	552	552	552	552	690	690	353	270	264,1	552	552
Young's modulus	GPa	206	206	206	206	206	206	206	206	70	65,5	206	206
Poisson's ratio	–	0,30	0,30	0,30	0,30	0,30	0,30	0,30	0,30	0,32	0,33	0,30	0,30
Unsupported length	mm	641	615	784	345	430	588	736	365	34,5	48	754	722
Mean radius	mm	3013	3114	4218	2811	3514	2813	3516	1549	111,4	121,5	2540	2700
Shell area	mm^2	16,900	16,875	28,800	7920	12,150	15,600	24,000	6750	108	150	19,355	18,250
Effective ring area	mm^2	6135	6153	14,578	4730	9141	4784	8717	1843	42	34	3383	2945
Ratio area shell/area ring	–	2,75	2,74	1,98	1,67	1,33	3,26	2,75	3,66	2,57	4,38	5,72	6,20
Young's modulus/Yield stress	–	373	373	373	373	373	299	299	584	259	248	373	373
Shell flexibility parameter θ	–	2,94	2,73	2,59	1,78	1,79	2,79	2,82	2,81	2,55	3,21	3,82	3,57
Composite geometric parameter S	–	1,74	1,62	1,53	1,06	1,06	1,66	1,67	1,66	1,51	1,90	2,26	2,12
Batdorf parameter Z	–	5,00	4,29	3,86	1,84	1,86	4,51	4,59	4,56	3,75	5,97	8,40	7,37
Asymmetric buckling pressure p_e	MPa	8,41	9,41	9,86	14,29	13,64	10,34	9,91	16,22	27,60	19,73	8,07	7,50

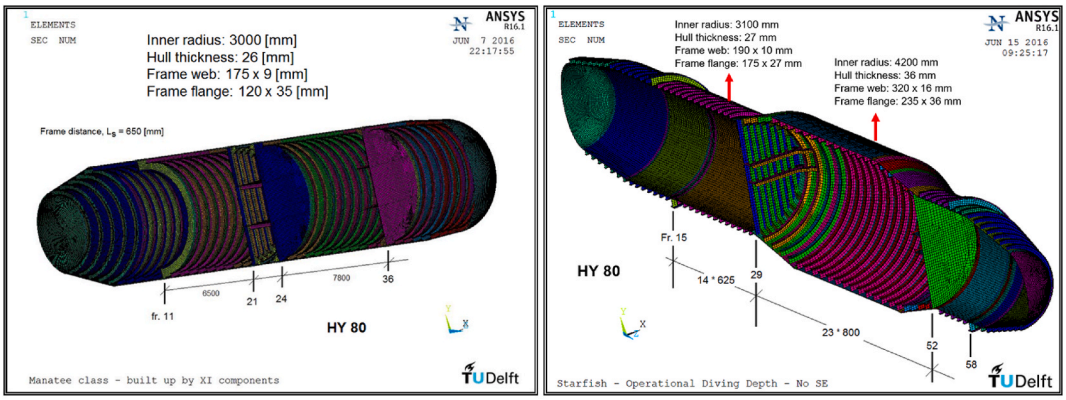

(a) Manatee class [41] [14] (b) Starfish class, Author's design

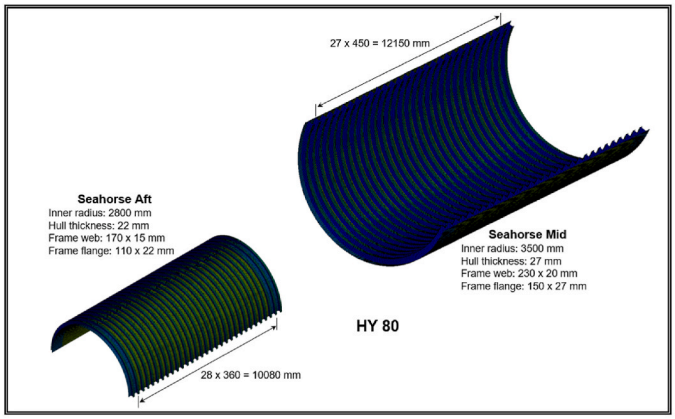

(c) Seahorse class, Author's design

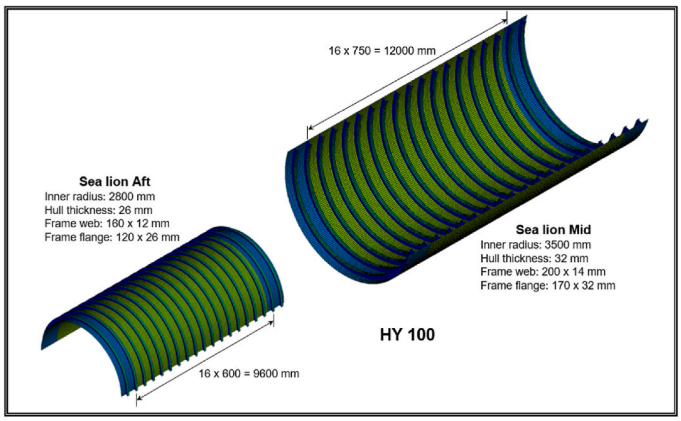

(d) Sea lion class, Author's design

Fig. A.1. Representative pressure hull geometries [14,41].

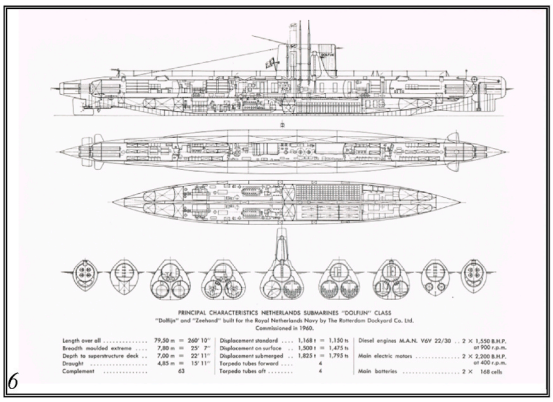

(a) Potvis class [42]

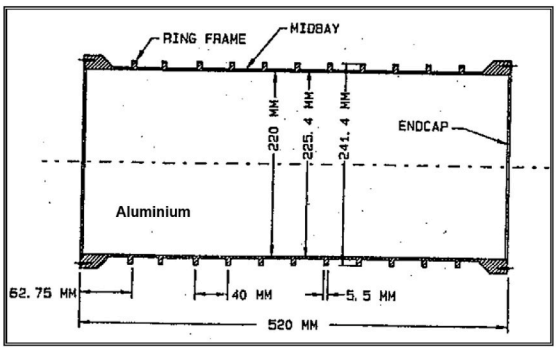

(b) DREA experiment [43]

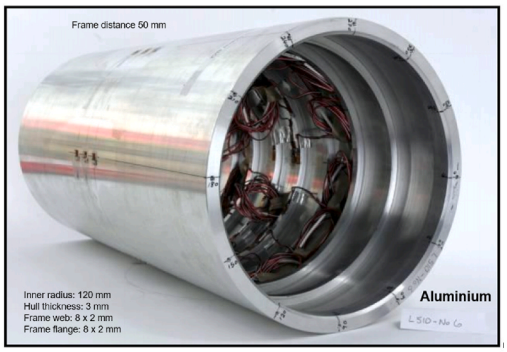

(c) ISSC Round robin [44] [45]

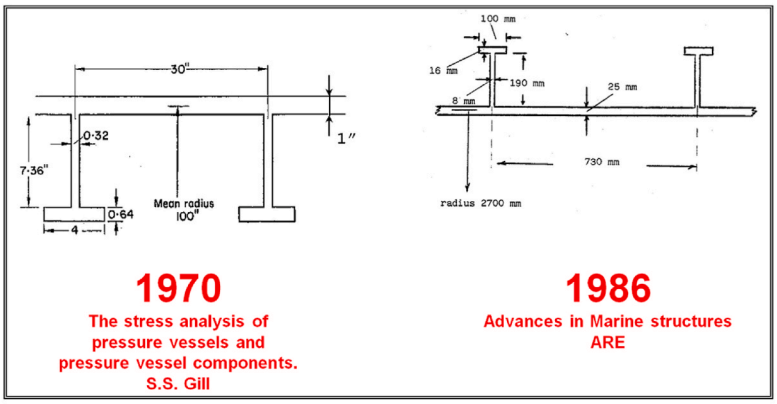

(d) Kendrick [21] [46]

Fig. A.2. Additional pressure hull geometries [21,42–46].

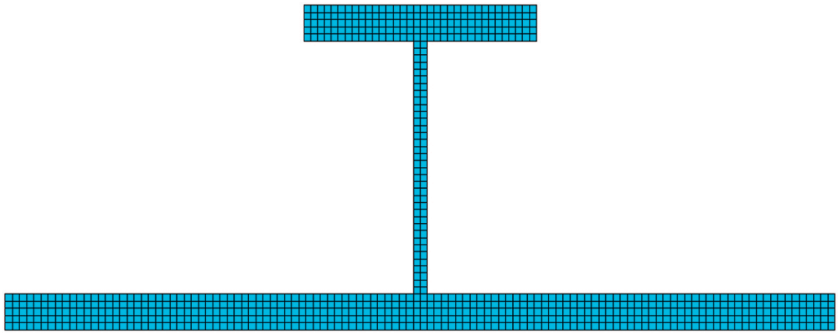

Fig. A.3. Example of the FE mesh – Starfish aft.

References

[1] ISSC 2018 Committee IV2. In: Proceedings of the 20th international ship and offshore structures congress, vol. 1. IOS Press; 2018.
[2] Vucinic B. MA-CAD, maintenance concept adjustment & design. Delft University of Technology; 1994.
[3] Stambaugh KA. On ship structure risk and total ownership Cost management assisted by prognostic hull structure monitoring. Delft University of Technology; 2020. https://doi.org/10.4233/uuid:3609236e-ec53-4157-9cdc-e461a9297b71.
[4] MacKay JR. Structural analysis and design of pressure hulls : the state of the art and future trends. Def. R&D Canada – Atl 2007:118.
[5] Reijmers JJ, Nobel P. The relevance of analytical formulations predicting stiffener tripping. NAFEMS World Congr 2021.
[6] Germanischer Lloyd. III rules for classification and construction, Part 1 underwater technology, chapter 2 submersibles. 1998.
[7] Pulos J, Salerno V. Axisymmetric elastic deformations and stresses in a ring-stiffened, perfectly circular cylindrical shell under external hydrostatic pressure. David Taylor Model Basin report 1961;1497.
[8] Lunchick ME, Short RD. Behavior of cylinder with initial shell deflection: David taylor Model Basin report report 1150. 1957.
[9] Bodner SR, Berks W. The effect of imperfections on the stresses in a circular cylindrical shell under hydrostatic pressure. 1952. PIBAL report 210, Polytechnic Institute of Brooklyn. N.Y.
[10] Kendrick SB. The deformation under external pressure of nearly circular cylindrical shells with evenly spaced equal strength nearly circular ring frames, Naval Construction Research Establishment report R259. 1953.
[11] Galletly GD, Bart R. Effects of boundary conditions and initial out-of-roundness on the strength of thins-walled cylinders subject to external hydrostatic pressure. David Taylor Model Basin Report 1957;1066.
[12] Reijmers JJ, Vlasman AA. Comparison FE codes, Nevesbu report 0-SR-1200-001. Alblasserdam 2016.
[13] MacKay JR, Jiang L, Glas AH. Accuracy of nonlinear finite element collapse predictions for submarine pressure hulls with and without artificial corrosion damage. Mar Struct 2011;24:292–317. https://doi.org/10.1016/j.marstruc.2011.04.001.
[14] Reijmers JJ, Stapersma D. Uncertainty quantification with respect to global collapse of submarine pressure hulls compared to interframe collapse. Stockholm: NAFEMS World Congr.; 2017.
[15] Batdorf SB. A simplified method of elastic-stability analysis for thin cylindrical shells I - Donnell's equation,. NACA Technical Note 1947;1341.
[16] Ellinas CP, Croll JGA. Elastic-plastic buckling design of cylindrical shells subject to combined axial compression and pressure loading. Int J Solid Struct 1986;22:1007–17.
[17] DNV-GL. Rules for classification, naval vessels, Part 4 sub-surface ships, chapter 1 submarines. 2018.
[18] PD5500. Specification for unfired fusion welded pressure vessels. British Standards Institution; 2018.
[19] DNV-GL. Fabrication and testing of offshore structures, Offshore Standards, DNVGL-OS-C401. 2017.
[20] von Mises R. Der kritische aussendruck zylindrischer rohre. Zeitschrift Des Vereines Dtsch Ingenieure. 1914. Band 58 Nr. 19.
[21] Kendrick SB. The stress analysis of pressure vessels and pressure vessel components. first edit. Pergamon Press; 1970. https://doi.org/10.1016/c2013-0-01596-4.
[22] Kendrick SB. Collapse of stiffened cylinders under external pressure. In: Proc. IMechE conf., vessel. Under buckling cond., London; 1972. p. C190/72.
[23] Faulkner D. The collapse strength and Design of Submarines. RINA – Nav. Submar., London. 1983. p. paper 6.
[24] MacKay JR. Experimental and numerical modeling in support of a structural design framework for submarine pressure hulls based on nonlinear finite element collapse predictions. Delft University of Technology; 2012.
[25] Cerik BC, Shin HK, Cho SR. Probabilistic ultimate strength analysis of submarine pressure hulls. Int J Nav Archit Ocean Eng 2013;(5):101–15. https://doi.org/10.3744/JNAOE.2013.5.1.101.
[26] Cho SR, Muttaqie T, Do QT, So HY, Sohn J-M. Ultimate strength formulation considering failure mode interactions of ring-stiffened cylinders subjected to hydrostatic pressure. Ocean Eng 2018;161:242–56.
[27] Lunchick ME. Yield failure of stiffened cylinders under hydrostatic pressure. David Taylor Model Basin report 1959;1291.
[28] Reynolds TE. Inelastic lobar buckling of cylindrical shells under external hydrostatic pressure. David Taylor Model Basin report 1960;1392.
[29] Lunchick ME. Plastic axisymmetric buckling of ring-stiffened cylindrical shells fabricated from strain-hardening materials and subjected to external hydrostatic pressure. David Taylor Model Basin report 1961;1393.
[30] Pulos J. Structural analysis and design considerations for cylindrical pressure hulls. David Taylor Model Basin report 1963;1639.
[31] Faulkner D, Das PK. Application of reliability theory to structural design and assessment of submarines and other externally pressurised cylindrical structures. Integr. offshore Struct 1991;4.
[32] Faulkner D. Application of reliability theory in submarines design. Adv. Mar. Struct 1991:566–95. 2, Dunfermline.
[33] Chryssanthopoulos MK, Baker MJ, Dowling PJ. Probabilistic buckling analysis of ring-stiffened cylinders. Adv Mater Struct 1991:608–27. 2, Dunfermline.
[34] Frieze PA. Reliability analysis in theory and practice. Adv Mater Struct 1991:596–607. 2, Dunfermline.
[35] Morandi AC, Das PK, Faulkner D. Reliability based design of submersibles: an investigation on the general instability of externally pressurised cylindrical vessels. OMAE - 1993;II:297–304. Saf. Reliab.
[36] Groen HTF, Kaminski ML. Optimisation of pressure vessels under reliability constraints. In: Proc. 15th Int. Conf. Offshore mech. Arct. Eng. OMAE, Florence; 1996.
[37] von Mises R. The critical external pressure of cylindrical tubes under uniform radial and axial load. Translation report 1933;366. United States Experimental Model Basin. 1929.
[38] Bryant AR. Hydrostatic pressure buckling of a ring-stiffened tube. Naval Construction Res Establish Rep 1954;306.

[39] von Sanden K, Günther K. The strength of cylindrical shells, stiffened by frames and bulkheads, under uniform, External pressure on all sides: translation, vol. 38; 1952. by David Taylor Model Basin. 1921.
[40] Wilson LB. The elastic deformation of a circular cylindrical shell supported by equally spaced circular ring frames under uniform external pressure. Trans RINA 1966;108.
[41] Reijmers JJ. Reliability based pressure hull design. 2015. NAFEMS World Congr., San Diego.
[42] Potvis. Grootspant onderzeeboten potvis-klasse, tek. Z-4, rev B. 1966. https://www.marinemuseum.nl/nl/collectie/museumschepen/.
[43] Bosman TN, Keuning PJ. Pegg NG. Experimental and numerical determination of the non-linear overall collapse of imperfect pressure hull compartments. Warsh 1993;93:13.
[44] Mackay JR, Pegg NG. Case study : submarine pressure hull collapse ISSC committee V. 5 naval ship design, technical note DRDC atlantic TN 2010-190. 2010.
[45] ISSC Committee V.5. In: Proceedings of the 18 Th international ship and offshore structures congress, One; 2012.
[46] Kendrick SB. Design of submarine structures. Adv Mater Struct 1986. Dunfermline.